

Acoustic detection of invisible damage in aircraft composite panels

L.P. Dickinson^{a,1}, N.H. Fletcher^{b,*}

^a CSIRO Industrial Physics, P.O. Box 218, Lindfield NSW 2070, Australia

^b Research School of Physical Sciences and Engineering, Australian National University, Canberra ACT 0200, Australia

Received 14 August 2007; received in revised form 13 December 2007; accepted 31 December 2007

Available online 21 February 2008

Abstract

The wing and body panels of modern commercial and military aircraft often consist of a three-layer structure in which two thin skins of fibre-reinforced composite or of aluminium are held apart by a much thicker core consisting of a honeycomb structure made from either folded paper-like material impregnated with aramid resin or from thin, folded aluminium sheet. A major maintenance inspection problem arises from the fact that impact by a heavy soft object has the potential to deflect the skin and damage the core, after which the skin can return to its original shape so that the defect is nearly invisible. This paper gives details of an acoustic inspection system that can reveal such damage and provide information on its nature and size using a hand-held “pitch-catch” device that can be scanned over the suspected area to produce a visual display on a computer screen. The whole system operates in the frequency range 10–30 kHz and embedded programs provide optimal examination procedures.

Crown Copyright © 2008 Published by Elsevier Ltd. All rights reserved.

PACS: 43.40.Le; 43.40.Dx; 81.70.Bt; 43.40.–r

Keywords: Aircraft panels; Impact damage; Acoustic inspection

1. Introduction

Modern commercial and military aircraft often employ a three-layer sandwich construction for both wing and fuselage panels in order to maximise functionality and strength while minimising weight. A typical sandwich panel consists of two stiff skin layers 1–5 mm in thickness separated by a light core 10–50 mm thick. These panels usually have skins formed from laminated multi-ply composites of either carbon-fibre or fibre-glass in a matrix of polymer resin, although other skin materials such as aluminium are sometimes used. Sandwich panel cores are stiff, light-weight, and are usually either a honeycomb structure or a closed-cell foam. A very common core used in modern aircraft, commercially known as Nomex, is made from a

paper-like material folded into a honeycomb shape and impregnated with an aramid resin to add strength, though some panels use aluminium for cores as well as for skins.

Composite sandwich panels are very effective in terms of strength-for-weight, but can suffer from a potentially serious problem. If the panel is subjected to an impact by a low velocity object such as a worker’s dropped tool, or even something soft such as a tyre fragment thrown up from the runway or collision with a bird in flight, then the skin at the impact site can be deflected inwards without noticeable cracking and cause crumpling or fracture within the core, as shown by the example in Fig. 1. After the impact the skin is free to restore itself back to its original shape so that the damage can be almost invisible. This form of damage is often referred to as Barely Visible Impact Damage, or BVID. Even a relatively small amount of crumpling of a honeycomb core can significantly affect the local stiffness of the panel, so that it is desirable to identify any instances of impacts and verify that the structure is still adequately load-bearing.

* Corresponding author. Tel.: +61 2 6125 4406; fax: +61 2 6125 0511.
E-mail addresses: laurence.dickinson@csiro.au (L.P. Dickinson),
neville.fletcher@anu.edu.au (N.H. Fletcher).

¹ Tel.: +61 2 9413 7541; fax: +61 2 9413 7200.

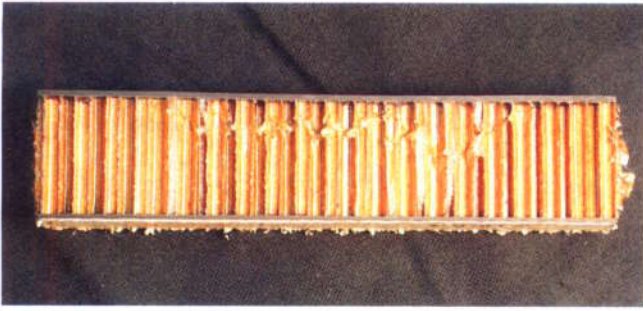


Fig. 1. Cross-section showing damage in a panel with 1.6 mm fibre-reinforced skins and 24 mm Nomex core after impact by a rubber-tipped metal “tup” of mass 2 kg and diameter 25 mm dropped from a height of about 1 m. Damage from such an impact typically begins for a drop height of about 50 cm. Note the irregularity of the damage depth.

Traditionally the most common method for inspection of aircraft used to be visual inspection by ground staff, with light tapping of any suspected areas with a hard, blunt instrument to give an indication of the underlying structure from the sound of the tap. This is called a “coin tap” test and, although originally subjective as the name implies, was later developed into an automated analysis system. This automated system involves a controlled light impact on the panel, with monitoring of both impact force and panel deflection as functions of time to give a measure of its local mechanical stiffness [1]. Other methods have been also been devised to inspect aircraft, such as the use of X-rays, thermography, dye-penetrants, eddy current measurements, shearography, and magnetic particles [2] but by far the most commonly implemented methods for testing composite panels are those using acoustic techniques.

It might have been expected that the best way to examine composite panels would be to use ultrasound, and much has been published on ultrasonic techniques [3], but the great difference in acoustic impedance between the skin and core creates considerable difficulties and, in addition, it is often not possible to access both sides of an assembled panel to utilise through-transmission techniques. This has led to the development of techniques for lateral wave propagation measurements at lower frequencies. One such family of commercially available acoustic sensors, developed in the 1980s, is called “pitch-catch” probes [4]. Unlike ultrasonic techniques, the basic operation of acoustic pitch-catch probes, originally developed by Lange [5,6] in Russia, has received relatively little recent published attention, although there are several commercial embodiments of the technique available. What is presented has usually been empirical in nature, rather than addressing basic issues. Recently CSIRO in Australia has developed an extended version of an acoustic pitch-catch probe housed within a hand-held device named the “Bandidoot” after a small Australian marsupial animal with a long sensitive nose that it uses to detect small insects for food. The name, when written “baNDIcoot” also incorporates the acronym “NDI” for “Non-Destructive Inspection”. This instrument and its associated software are

attracting considerable interest from aircraft manufacturers and operators around the world. The present paper aims to provide some insight into the manner in which such probes operate and to show how different types of damage can be located and identified.

2. Waves and vibrations in composite panels

The transducers used in the baNDIcoot are sensitive only to vibrations normal to the panel surface, but there are several types of vibrational waves that can contribute to this motion. Let us consider these wave types in turn. All are complicated by the fact that the panel is not a simple plate of uniform composition but contains a light core sandwiched between its two skins. Even for a homogeneous plate, the detailed equations of motion are extremely complicated if the wavelength is not long compared with the plate thickness [7], and analysis of a composite panel is more complex even if this simplifying assumption can be made [8], but an adequate approximation has been given by Thwaites and Clark [9].

Under transverse stress the panel will deform in whichever way requires least elastic energy. If the wavelength is greater than about five times the panel-thickness, then the panel deforms by bending. It is this sort of deformation that the panels are designed to resist, the two skins providing a large stiffness against the stretching and compression necessarily involved in the wave, with the core serving to hold the skins apart and so magnify the effect. If the skin thickness is h and the core thickness H and we make the assumption that the Young’s modulus of the core material is essentially zero in the plane of the core but large in the normal direction, then bending waves simply stretch or compress the skins, with their separation remaining constant. To a first approximation the bending stiffness is then $E_s h H^2 / 2(1 - \sigma_s^2)$, where E_s is the Young’s modulus for stretching of the skin in the surface plane and σ_s is its Poisson’s ratio, while the moving mass per unit area is $\rho_s h + \rho_c H$, where ρ_s is the skin density and ρ_c is the density of the core. Solution of the standard bending wave equation then gives the speed of a bending wave of angular frequency ω as

$$c_b \approx \omega^{1/2} \left[\frac{E_s h H^2}{2(1 - \sigma_s^2)(\rho_s h + \rho_c H)} \right]^{1/4}, \quad (1)$$

Note that the speed of these bending waves increases proportionally to the square root of the frequency.

If the wavelength is less than about five times the panel-thickness, then the deformation becomes a shear wave in the panel. The shear stiffness is simply the combined stiffness of core and skins, and the mass is also the combined mass, and the speed of shear waves is thus

$$c_s \approx \left(\frac{G_c H + 2G_s h}{\rho_s h + \rho_c H} \right)^{1/2}, \quad (2)$$

where G_c is the shear modulus of the core and G_s that of the skin. The propagation speed in this case is independent of frequency.

Both bending and shear waves are really limiting cases of the actual wave behaviour in the panel, which always involves a little of each type, though with one or other type of deformation being dominant in the different wavelength regimes. In addition, each wave may involve a shear distortion of the core coupled to a bending distortion of the skins, which leads to further theoretical complications. The vibrational wave velocity in aircraft panels of interest is of order 500 m s^{-1} and the panel-thickness typically 10–50 mm, so that the bending/shear cross-over frequency will be in the range 2–10 kHz. Since nearly all measurements are made at frequencies higher than this, the waves are predominantly of the shear rather than bending type.

The third significant type of wave is compressional and propagates through the thickness of the panel normal to the surface at speed

$$c_c \approx \left(\frac{E_c}{\rho_c} \right)^{1/2} \quad (3)$$

where E_c is the Young's modulus of the core material in a direction normal to the panel surface. At low frequencies this vibration does not propagate away from its source as a wave but is localised as a standing wave across the panel-thickness until its first resonance frequency is exceeded. Above this frequency it can couple to other waves and propagate away from its source in a lateral direction.

A point source such as is used in pitch-catch probes will excite all of these wave types in an intact panel, but the one of most interest at the frequencies used is a shear wave with a small component of bending strain. This wave propagates at a speed typically in the range $300\text{--}500 \text{ m s}^{-1}$ nearly independently of frequency, the exact value depending upon the panel material and structure. For completeness it should be noted that there are other wave types, both longitudinal and transverse, that can be generated by an excitation source that can apply a force parallel to the panel surface, but these are not relevant to the present discussion.

3. Damage detection methods

There are several approaches to damage detection that use waves in the sonic regime below about 20 kHz, though these have now been extended up to about 50 kHz as will be discussed later. The first to be discussed is a laser system, developed by Suzanne Thwaites and Norman Clark of CSIRO [9–11] in which the panel to be tested is excited by a mechanical shaker and a laser beam is scanned over its surface to measure the phase, and thus the propagation velocity, of waves at the selected frequency. Since any defect will influence the local mechanical properties of the panel and thus the wave velocity, this method reveals hidden impact damage. While this method is good for examining flat panels before assembly, it is difficult to adapt it to

measurements on assembled aircraft structures, though developments using an oscillating air jet in place of a mechanical shaker provided some advantage.

A more direct method is to measure the mechanical impedance of the panel at points over its surface. Mechanical impedance is defined as the ratio of force to velocity at a given frequency, and such a measure will certainly be different over a defect to its value on intact panel. The normal measurement method involves using an electro-mechanical vibrator that is brought into contact with the object under test through an impedance head that measures both applied force and panel acceleration. The acceleration signal can then be integrated to give velocity. A modification of such a device called an "MIA" or Mechanical Impedance Analysis probe, which uses two piezoelectric elements mechanically in series, is in common use. The upper element acts as a driver and the lower one detects a quantity related to the displacement of the panel. The two signals can then be combined and frequency-weighted to give an approximation to the mechanical impedance at that point. When an appropriate measurement frequency has been determined, this sensor can be scanned by hand across the panel to give time-resolved measurement of mechanical stiffness, as has already been referred to [1].

A closely related method that is easier to implement separates the excitation point from the measurement point by a small distance and uses an identical piezoelectric reversible activator/sensor for each. For obvious reasons such a device is called a "pitch-catch" probe and various versions are commercially available. The actual sensor can be made quite small, about the size of a computer mouse, and is easily scanned by hand over the panel being examined. The activator and sensor, which are typically separated by 10–15 mm, make contact with the panel through short pins and are often spring loaded to maintain contact, the whole probe being positioned a little above the panel surface using plastic sliders. Two examples of such probes currently available can be found in the Olympus Bondmaster and the Zetec Sondicator. The sensor is connected to an electronic system that generates the probe signal and processes the output. One advantage of this device over the single-point impedance probe is that the phase difference between the signals at the pitch and catch pins provides information about the propagation velocity of the waves involved over the length of panel between them, and this can be useful in characterising any defect.

Nelson et al. [12] recently developed a resonance approach to panel inspection based upon use of a pitch-catch probe. An intact panel will have a transverse resonance behaviour associated with compressive waves, and the frequency of such resonances and anti-resonances will be determined by the mass of the skins and the thickness and elasticity of the panel core. Their approach was to use a continuous probe signal adjusted to match the frequency of either a resonance or an anti-resonance of the intact panel under test. Defects in the panel core caused

by impact damage or other factors then show up as regions of high contrast in the resultant displayed image.

The baNDIcoot, shown in Fig. 2, is an independent development of the pitch-catch probe, carried out by Laurence Dickinson and Suzanne Thwaites of CSIRO [13,14] over the past ten years and involving modification of both the probe head itself and also the techniques used for damage detection. This new sensor has many advantages over other versions. From a physical point of view, the structure of the connecting pins and their attachment to the transducers has been modified to remove structural resonances so that the frequency spectrum up to 50 kHz is available for measurement. A laser-illuminated optical sensor, a commercial product of Agilent Technologies [15], has also been included. This captures 2000 images a second and, by comparing successive images, identifies the position of the sensor on the panel with an accuracy of better than 1 mm. This allows an accurate screen display of the panel under examination to be produced. Finally, sophisticated software has been developed to produce a wide variety of probe signals and to allow processing of the detected signals in both time and frequency domains. Stored analysis programs allow simple selection of the protocol to be used, and the result is a colour image displayed on a computer screen and accompanied, if desired, by an audio alert signal.

All the software for operation of the scanner can be loaded onto a portable computer, which will then display the scan results. All that is required is a USB connection to the hand-held scanner to provide DC power and communicate the information. The computer can then be used to vary the scan parameters. Standard programs typically use either a pulse of three to five cycles of a sinusoidal

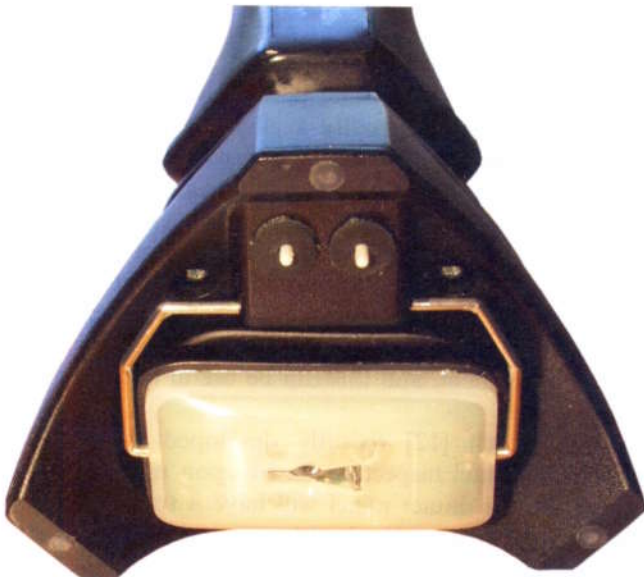


Fig. 2. The underside of the baNDIcoot scanner showing the two small white pins of the “pitch” and “catch” transducers and the large white optical positioner. Three small stabilising buttons are located towards the corners of the probe. This scanner head is mounted on a handle which allows convenient hand movement over the panel under inspection.

waveform, generally with a fundamental frequency somewhere in the range 10–30 kHz, or else a swept-frequency chirp signal or a saw-tooth wave covering a wider range. For analysis, a signal of about 1 ms duration is captured, and this is displayed along with its frequency analysis. Most importantly, however, there is a full-colour spatial display of the results of the scan, as shown for example in Fig. 3. Since the duration of the recorded waveform is about 1 ms, while even a five cycle pulse at 20 kHz lasts only 0.25 ms and takes only about 0.02 ms to propagate

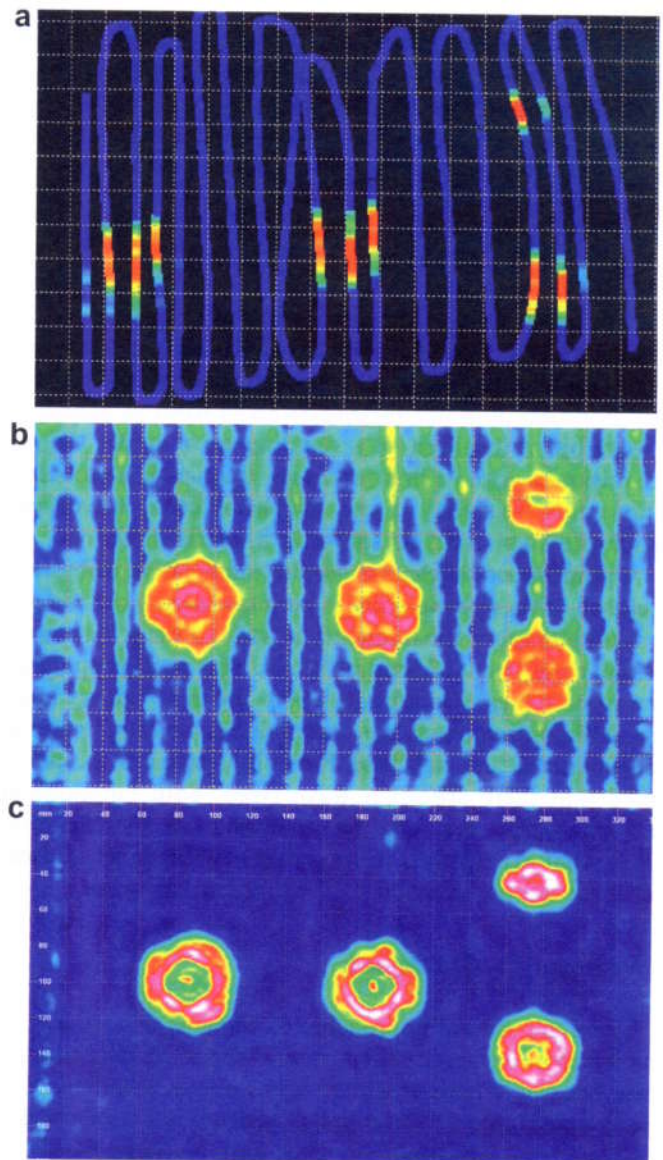


Fig. 3. (a) Broadband exploratory “chirp” scan of a 24 mm Nomex test panel with 1.2 mm skins containing several damage sites caused by impact of a 14 mm soft impact device or “tup”. (b) Complete scan of the Nomex test panel. The quantity plotted is the integrated difference between the sample spectrum and a reference spectrum from a point on undamaged panel. Red indicates maximum amplitude and blue minimum amplitude. The vertical blue bands are artifacts rather than damage and can be removed by a band-stop filter at 17 kHz, as shown in (c). Scan dimensions are approximately 340×200 mm.

from the pitch pin to the catch pin, the analysis is only partly of the directly propagating wave and much of it examines the subsequent reverberant vibration. The analysis window can be placed anywhere within the 1 ms time interval and its position and length can be adjusted to highlight local defect information. Alternatively, the whole signal duration can be used and a particular frequency band chosen for display in the analysis. One additional analysis ability available is to compare the probe response over a suspected damage area with that for the intact panel. To do this, a stationary measurement is made in a region of the panel known to be free from defects and the result is stored. Every analysis pixel of the scanned image can then be compared with this stored standard and only differences displayed.

Since examination on actual aircraft is usually carried out by hand, it is important that damage can be detected easily and quickly. Fig. 3a shows a rapid hand-scan over a damaged panel from which it can be seen that the damage is easily identified and localised for more detailed scanning. It is then possible to move the scanner repeatedly over the damaged areas to produce a detailed scan. For the purposes of the present paper, however, a mechanical scanning system was used to produce complete scans such as that shown in Fig. 3b. In such scans the colour indicates the amplitude of the vibrational response, red being a maximum and blue a minimum. The defects in this panel, produced by dropping a soft weight onto it, are clearly visible. The vertical blue bands are artifacts, mostly due to standing waves, as will be discussed in detail in Section 9.

4. Scan resolution

Since the two contacts of the sensor are about 12 mm apart, it is reasonable to expect that this sets the resolution of the image. While this is generally correct, there are some interesting sidelights. One of these is that some settings of the program parameters can actually display an image of the underlying core despite the fact that the cell size is less than half the pin separation on the scanner. It is helpful to discuss how this can occur, since it is also relevant to the imaging of small defects.

Suppose that the pin separation on the scanner is an integer multiple of the core cell size. Then in some positions of the scanner both pins will be over the walls of core cells, while in other positions they will both be over the centre of a cell. The resulting signal in these two cases should certainly be different and this would explain the resulting core image. Suppose, however, that the pin separation is not a simple multiple of the core cell size. There are then two possibilities: either one of the pins will be over a cell wall and the other over a cell interior, or else both will be over cell interiors. Again, we should expect the output signal for the two cases to be different, but a result called the reciprocity principle tells us that the result when one pin is over a wall and the other over a cell interior should be the same no matter which of the two is the pitch and which the catch

pin. What this means is that the output screen effectively displays two superimposed images of the core which are separated by a distance equal to the pin spacing. This is of no real concern but explains this apparent resolution anomaly.

Something similar can occur in images of very fine structures such as line defects, which may appear as two slightly separated parallel lines. Since, however, the resolution of the display is normally set to about half the pin spacing, these two lines will normally overlap so that, overall, the resolution achieved by the sensor is about half its pin spacing, and so about 6 mm.

5. Revealed defect structures

There are many kinds of defect that can be produced in composite panels. The two most relevant to the purposes for which the baNDIcoot is applied are defects within the panel, such as an area of crushed core caused by a soft impact as shown in Fig. 1, or a skin delamination typically resulting from a manufacturing defect. It is therefore appropriate to look briefly at the response to be expected in these two cases.

For most of the frequency range used in measurements, the wavelength is much greater than the thickness of isolated skin, so that waves in disbonded skin will be of the bending variety. Measurements on typical skins and panels show that the phase velocity of waves on isolated skin is usually less than that of waves in the intact panel over the range 10–20 kHz. For a three-ply skin alone the phase velocity is about 250 m s^{-1} at 10 kHz and about 400 m s^{-1} at 20 kHz, while that in the honeycomb sandwich panel with this skin varies between 400 and 600 m s^{-1} depending on propagation direction. In the case of a disbond or core crush in such a panel, most of the effective core stiffness is lost, so that there is a similar discrepancy in wave speed within the defect region. It is this fact that provides the basis for defect detection within the high audio-frequency range, since the wavelength in the defect region is comparable with the size of defect.

Fig. 3b shows a scan of a 24 mm Nomex panel containing impact damage and examined with a probe signal consisting of a swept-frequency “chirp” with parameters set to emphasise the 10–20 kHz band. This broadband scan protocol is designed to detect damage of all types and can be subsequently refined to examine details. For some of the damage regions shown in this scan the rear skin has been subsequently removed, which makes very little difference though the scanner display parameters can be set to make it visible.

6. Crushed core

The essence of a crushed core defect is that an impact can depress the skin at the impact site by an amount sufficient to cause a crumpling failure of the core matrix, as shown in Fig. 1. After the impact the skin may return to

nearly its original shape, so that the defect is almost invisible, but the crushed core will introduce significant structural weakness. A major purpose of the acoustic scanning technique is to detect such defects.

If the impacting object is small or curved, then the stress in the core will be greatest near the impacted skin. There is, however, some extra strength in the core very close to the skin because of the adhesion process, so that core failure takes place a small distance inwards from the impacted side. In typical cases where the impacting object is curved, the failure occurs at about one quarter to one third of the core depth. The shear strength of the core plus skin is therefore reduced to less than half of its original value on the impact side and by a smaller amount on the other side. The mass of skin plus core is similarly reduced, but is more nearly one half on each surface of the panel since much of the mass resides in the skin. The net result is therefore a decrease in shear wave speed over the impact site on the impact side. There will be a related change in speed on the other side of the panel, but this is not of practical importance since this side is generally not available for scanning on an aircraft. The propagation speed of any bending component in the wave will, however, decrease much more notably, since bending stiffness in the remaining core is proportional to the cube of its thickness. The effect of this will be to increase the magnitude of the bending component of the wave within the defect and thus to decrease the wave velocity even further and in a frequency-dependent manner. The other effect of the impact will be a large change in the compressive component of the vibration produced by the probe. In fact the compressive stiffness of the core in the defect region will be almost zero, so that the compressive wave can be ignored and attention focussed on the uncoupled motion of the skin and attached core on the impact side.

Because of the large decrease in wave impedance of the defect relative to the surrounding panel, and since its size is generally comparable with the wavelength of the probing signal in the surrounding panel, it is simplest to treat the defect as a nearly isolated resonant structure with a boundary that is not completely rigid. We can then simplify matters even further by taking the boundary to be actually rigid, since the vibrational modes inside the defect are then well known [16,17] and can be described in terms of nodal circles and nodal diameters. If the number of nodal circles, counting the one at the edge, is denoted by n and the number of nodal diameters by m , then the modes can be labeled (m,n) and their relative frequencies $f(m,n)$ are approximately as shown in Table 1. The frequencies for bending modes are more widely spread than for shear modes, and none of the frequencies are in simple harmonic relation. If the boundaries of the defect are not rigidly clamped, as is certainly true in practice, then the mode frequencies will differ somewhat from the values shown here.

To a first approximation, the accuracy of which increases for higher modes, the frequency of bending modes behaves as

Table 1
Relative mode frequencies

Relative mode frequencies $f(m,n)$ for bending vibrations		
$f(0,1) = 1.0$	$f(0,2) = 3.9$	$f(0,3) = 8.7$
$f(1,1) = 2.1$	$f(1,2) = 6.0$	$f(1,3) = 12$
$f(2,1) = 3.4$	$f(2,2) = 8.3$	$f(2,3) = 15$
Relative mode frequencies $f(m,n)$ for shear vibrations		
$f(0,1) = 1.0$	$f(0,2) = 2.3$	$f(0,3) = 3.6$
$f(1,1) = 1.6$	$f(1,2) = 2.9$	$f(1,3) = 4.2$
$f(2,1) = 2.1$	$f(2,2) = 3.5$	$f(2,3) = 4.8$

$$f_b(m, n) \propto \left(n + \frac{m}{2}\right)^2, \quad (4)$$

while that of shear modes behaves as

$$f_s(m, n) \propto n + \frac{m}{2} - \frac{1}{4}. \quad (5)$$

From this it can be deduced that the density of modes as a function of frequency is about proportional to $f^{1/2}$ for bending modes and proportional to f for shear modes. The mode spacing within this general pattern is, however, rather irregular.

The frequency $f(0,1)$ of the first mode, and therefore of all the higher ones, is inversely proportional to the defect diameter in the case of shear distortions and inversely proportional to the square of the diameter for bending distortions. The fact that there is usually a significant thickness of core adhering to the skin on the impact side stiffens it, making its vibrations essentially shear in nature. In general, larger defects will have a thicker layer of adhering core, adding considerably to its stiffness but only a small amount to its mass, so that the frequency range as a function of defect size will be compressed compared with the simple picture presented above. Because of rather large losses in the fractured core, the quality factor or Q-value of the defect resonances will not be large, so that each can be excited over a considerable frequency range. This results in a large overlap of neighbouring modes, particularly at higher frequencies, so that the resulting vibration patterns will not be as well defined as expected from simple theory but will tend to a general circular symmetry. At high frequencies, in addition, irregularities in the fractured core, such as those in Fig. 1, may become visible.

These predictions can be verified to some extent by analysing the received signal from the broadband baNDIcoot scan of Fig. 3 in particular narrow frequency bands, as shown in Fig. 4. It should be noted that, because the exciting tip of the probe is moved over the panel to produce the scan pattern, this will generally cause a related rotation of the angular pattern of each mode, so that we should not expect the angular symmetry, encoded in the parameter m , to be as pronounced as is the radial symmetry, encoded in the parameter n .

In the lowest frequency band, 5.5–6.5 kHz, the $(0,1)$ mode is the one excited to largest amplitude so that the vibrational pattern has a simple maximum at its centre as

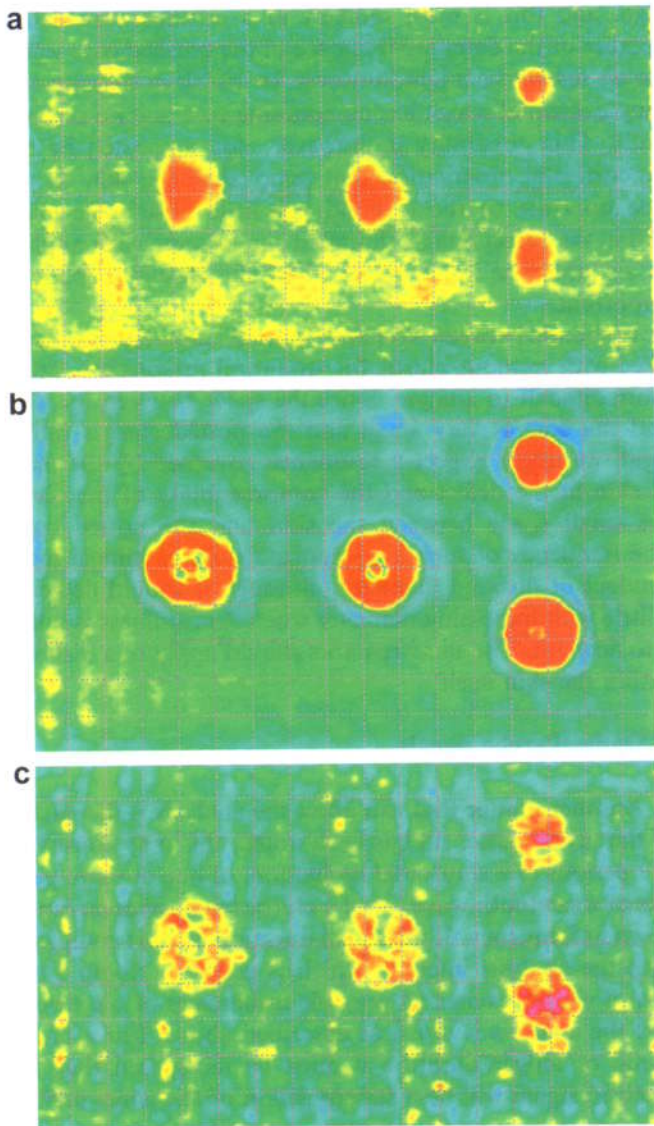


Fig. 4. The broadband excitation scan of Fig. 3, analysed in narrower frequency bands to show up dominant defect mode structures: from the top (a) 5.5–6.5 kHz, (b) 11–12 kHz, and (c) 20–22 kHz.

expected. The actual mode frequency may be less than this, the shift being due in part to the envelope of the signal frequency. In the next band, 11–12 kHz, the pattern closely resembles the superposition of the (0,2) and (2,1) modes, the latter being most obvious in the defect on the left. The apparent angular variations are probably interactions with the standing wave pattern along the panel rather than distinction between the two angular modes $\cos 2\theta$ and $\sin 2\theta$. In the highest frequency band shown, 20–22 kHz, several neighbouring modes are excited, but the dominant ones appear to be (0,3) and (2,2) as expected. The irregularity of the pattern is presumably due to corresponding irregularity in the crushing of the core, as in Fig. 1. Note that the mode structure in the small defect towards the top right corner is simpler than that of the larger defects. This is what is to be expected from the fact that mode fre-

quencies vary about inversely with the impact diameter so that the (0,1) mode of the small defect is excited over a higher frequency range than for the large defects. The fact that the observed frequencies of these modes are relatively small multiples of the frequency of the fundamental (0,1) mode near 6 kHz, the (0,2) mode being near 14 kHz, confirms that the defect vibration may predominantly involve shear rather than bending distortions, as can be seen from the figures of Table 1. This cannot, however, be taken as a defining feature, since it will depend upon the nature of the impact and the structural parameters of the panel.

Another question relevant to the detection of damage is the dependence of defect resonances on the skin thickness. To allow an appropriate test, a panel was obtained that had a set of defects consisting of circular spaces milled in the core during assembly, the defect diameters ranging between about 10 and 50 mm. In addition, the test panel repeats these defects over areas with different skin thickness, achieved by applying successive layers of thin fibre-reinforced sheet. Table 2 shows the measured major resonance frequencies for these defects, labeled from small to large by the letters A–D. There are two extra resonances at about 3 kHz and 20 kHz respectively but, since these are present in the intact panel sections as well, they are not included. The conclusion is that, while skin thickness has some effect on defect resonance frequencies, this effect is not large. It is also noticeable that, while defect size has about the expected effect on mode frequency for thin skins, this effect is reduced considerably for thicker skins. The explanation of these effects is not immediately clear, but it is noticeable that the apparent size of each defect increases with skin thickness, indicating a spread of vibration into the surrounding region of intact core.

Most test panels, and particularly those examined in Figs. 3 and 4, have well defined and realistic defect structures. Measurements show that the frequency at which damage is detected decreases with increasing defect size, as expected, but the rate of change, particularly for small defects, is much less than the inverse proportionality to the diameter expected from simple theory. There are probably several reasons for this. The first is that the depth of the core crush is not constant but varies with defect diameter, large defects having a greater depth of adhering core and therefore rather more stiffness. This follows from the fact that an infinitely large plane defect should have a core failure half-way between the two skins. The second reason is that the “catch” sensor of the probe has appreciable mass and stiffness, since it is spring loaded against the panel. The

Table 2
Resonance frequencies and skin thickness

	A (kHz)	B (kHz)	C (kHz)	D (kHz)
9 ply	14	12	9	6
13 ply	13	12	9	7
17 ply	12	11.5	9	7
21 ply	11.5	11	9	7
25 ply	10.5	10	9	7.5

frequency range of the measurements is, however, far above the initial resonance, so that the probe imposes a nearly fixed mass load on the panel. This has the effect of decreasing the resonance frequencies, particularly of the small defects where the load is comparable to or even greater than the defect skin mass. The result is that the prominent resonances of defects up to about 50 mm in diameter lie mostly within the 10–20 kHz range. This is convenient for the detection process, since it means that attention can generally be concentrated on this frequency band.

Most of these remarks apply also to scans made on the side of a test panel opposite to that of the impact, except that the skin is effectively rather stiffer because of the greater depth of adhering core. This should raise the frequencies of all the resonances by about the same factor, while amplitudes would be reduced.

This simplicity cannot, however, be expected in real-world impact damage caused by dropped tools, thrown stones, or collision with birds. These real impacts may produce damage that varies greatly in size and shape, and this will affect both the vibration patterns and the frequencies at which these will be excited. While the optimal examination frequency band within which many resonances of the defect will be excited can be expected to vary rather less than inversely with the linear defect dimensions, there will also be a significant dependence upon its shape. Despite these complications, it has proved possible to devise signals and analysis programs that give good detection sensitivity.

7. Disbonds

Another defect of importance is the “disbond”, generally a manufacturing defect in which the skin fails to adhere to the core, although there could also be a delamination within the skin itself, since it generally has several layers of fibres within its structure. In the case of a disbond between skin and core, the size of the defect is usually much greater than the thickness of the skin, so that skin deformation should be by bending rather than by shear. This will lower the frequency of the first resonance and, as indicated in Table 1, spread the resonances over a wider frequency range. This effect alone should make a visible distinction between disbonds and impact damage of similar size. There is, in addition, the possibility that the skin is still in contact with the core, though not adhering to it, for about half of each vibration cycle. This would affect the received signal by introducing higher harmonics of the probe frequency.

Since the skin on the probe side is set into vibration at much larger amplitude than the skin on the reverse side, this raises the possibility of resonances in the enclosed air columns of the core. The resonance of significance would have an integral number of half-wavelengths across the core thickness, so as to provide maximum stiffness, and this suggests a possible resonance for most panels in the range 10–20 kHz. For such a resonance to be visible, however, the Q-value of the air resonance would have to be very

high, and this is most unlikely in a crushed core defect because of the damping influence of the crushed core walls. An air resonance might, however, be visible in the case of a simple disbond which has no adhering core and no crushed walls. This possibility is, however, not supported by the experimental observation that removal of the skin on the side opposite to the disbond has little observable effect within the defect image, though it can be seen when applied to an otherwise intact panel where the elastic coupling is important.

Disbonds between skin and “potted” core that has been filled with resinous plastic for structural reasons are rather more difficult to analyse. Since the space between the skin and the core is very small and the potted core is rather rigid, we might expect a resonance governed by the mass of skin in the defect and the compressibility of the air in the small space between the skin and the potted core. The frequency of such a resonance would be almost independent of disbond diameter, although it should decrease a little with increasing diameter when skin stiffness is taken into account. The same remarks should apply to a disbond within the skin itself.

8. Optimal probe signals

Another matter that can affect the analysis is the nature of the probe pulse. As has been noted, this may consist of 2–7 periods of a sinusoidal oscillation, of one or more periods of a sawtooth wave, or of a chirp signal sweeping up or down in frequency. If the signal duration is short compared with the analysis interval, which is generally about 1 ms, then it simply excites all possible resonances of the defect, and the analysis is much as described above. For a probe signal of longer duration it must be recognised that the received signal will be a superposition of the panel oscillation and the propagating wave spreading from the pitch pin, since the edges of the defect are not completely rigid.

The simplest superposition case to consider is that of a continuous sine-wave oscillation of fixed frequency. This will initially excite the defect modes at their natural frequencies but will then drive them at the probe signal frequency with a phase shift between detected velocity and applied force somewhere in the range -90 to $+90^\circ$ depending upon whether the resonance frequency is below or above the probe frequency. The propagating wave will have a phase shift determined by the wave velocity, which is typically about 200 m s^{-1} in the defect region, and the distance between the probe pins, which is 12 mm. For zero phase shift, the two signals will be in-phase at a frequency around 17 kHz, and the phase differences will only shift this within the band 13–21 kHz. This is perhaps the reason that this band is preferred for sinusoidal probe signals extending over a large fraction of the analysis window time.

In the case of a probe signal of short duration, the analysis window may be located after the end of the probe signal. By this time the mode oscillations will have returned to their natural frequencies, but the oscillation amplitude of

each mode will be determined by the difference between its natural frequency and the exciting frequency. In one experiment a probe signal consisting of a 2-cycle sine pulse was used to examine impact defects with diameters in the range 10–30 mm in a 26 mm panel with 1 mm skins, and the effect of probe frequency was examined. A previous measurement showed that there was a prominent resonance, presumably (0,1) in the range 8–12 kHz, the larger defects having lower frequencies as expected. From Table 1, the (0,2) resonance frequencies should then be in the range 20–30 kHz. The pulsed probe signal produces a broadband excitation with most energy near the pulse frequency. The resulting scans for pulse frequencies of 11–15 kHz showed little difference, the pattern being that of a (0,1) mode for the smaller defects and a (0,2) mode for the larger ones, as might be expected. Excitation at 23 kHz excitation gave poorer defect resolution at all sizes, presumably because the modes of high visibility around 15 kHz were not greatly excited.

In the case of a chirp signal the situation is more complex and depends upon chirp direction and upon the rate at which the frequency is being swept, but this superposition effect may need to be taken into account in detailed considerations of the operation. Fortunately these matters are of no real practical concern, because analysis protocols that optimise detection sensitivity for particular situations have been developed experimentally and are made available as stored programs. The broadband chirp signal generally used for initial inspection sweeps linearly downwards over the frequency range from 25 kHz to 1 kHz, the signal duration is about 750 μs , and there is a windowing function to smooth signal onset and cessation. The result is a signal amplitude within ± 3 dB over the range 5–21 kHz. Optimised probe signals for particular applications can be developed, stored and used as new situations or products occur.

9. Artifacts

As well as patterns relating to damage in the panel, artifacts show up on some panels, such as the vertical blue bands in the broadband scan of Fig. 3b. Since these bands are sometimes observed also in intact panels they do not represent damage and, since they can be largely removed by applying a band-stop filter as in Fig. 3c, or by limiting the frequency range of the analysis, which is often desirable anyway, they are not of great practical concern. Nevertheless it would be good to know their origin.

While the artifact bands in Fig. 3b are largely vertical, it can be seen that there are less obvious bands oriented horizontally, both with a separation of about 20 mm. Both sets have the appearance of standing waves between the parallel edges of the test panel. Since the excitation is broadband, however, and the panel is long compared with the band separation, the question arises as to why a particular standing wave component should be emphasised. The solution appears to derive from the fact that, as well as waves prop-

Table 3
Artifact band separations

Panel-thickness (mm)	13.7	16.3	26
Skin thickness (mm)	0.8	1.5	1.6
Band spacing (mm)	8	12	15

agating parallel to the panel surface, there are also waves propagating across the panel-thickness and forming standing waves in this direction. Since the core thickness in this case is only about 22 mm, a wave velocity in the range 300–500 m s^{-1} would give a half-wave resonance lying in the frequency range 10–20 kHz, which is where the artifact bands are observed. If the displacement associated with standing shear waves along the panel for a particular frequency is in-phase with the displacement associated with the panel-thickness waves, then a bright band will result, while an anti-phase association will result in a dark band. The resonance of the transverse waves thus serves to determine the frequency, and thus the wavelength, at which standing waves along the panel are observed.

The obvious way to check this interpretation quantitatively is to examine similar artifacts in panels of different thickness. Since thicker panels generally have proportionally thicker skins, the shear wave velocity c_s given by (2) should be nearly unchanged, while the compressional wave speed c_c given by (3) is unchanged. Measurements on three panels showing these artifacts gave a band spacing approximately proportional to panel thickness, as shown in Table 3. The fact that these band artifacts are prominent on only some panels can be explained as the chance near-coincidence of the two resonance frequencies involved, while further support for this interpretation comes from the fact that the artifact bands disappear almost completely over regions of a test panel from which the rear skin has been removed, thus greatly modifying the compressive wave resonances.

10. Analysis protocols

If a panel is being inspected for unknown damage, then the initial strategy is to use a broad-band signal, such as the frequency-sweep chirp used to produce the results shown in Fig. 3, since this should interact with defects of all types. The received signal can then be analysed over several narrower bands to make particular defects more readily visible and to gain information about their nature. Other types of broad-band signal can also be used, such as short bursts of square or saw-tooth waves at a lower frequency. Once the preferred frequency band for detecting the defects has been identified, then they can be made more clearly visible, and unwanted artifacts removed, by using a probe signal of narrower bandwidth centred on the frequency of interest. This probe signal will generally consist of a burst of 3–5 periods of a sine-wave at the centre frequency, with some tailoring of the envelope through a filter window to reduce high frequencies. Since a particular baNDIcoot system will

generally be used repeatedly on aircraft of a particular type and searching for specific damage, several standard signals along with their most appropriate analysis protocols have been pre-programmed into the equipment, and an operator will normally select a particular one of these. New protocols can, however, be experimented with and stored for use.

For the scans reproduced in Figs. 3b and 4 above, the probe was carefully swept over the panel surface with a uniform spacing between sweeps. Such a procedure is not, however, necessary for manual scans in the field, and the probe can be swept in an arbitrary fashion across the panel as in Fig. 3a and then concentrated on areas where the display shows some sort of anomaly that might be a defect. Repeated passes over a single area do not affect the displayed result. The program then allows the resolution of the display to be varied to provide a smoothed image of such irregular manual scans.

11. Conclusions

Detection of manufacturing defects and impact damage in sandwich panels is a complicated matter because of the variety of different cases that can occur. The panels can vary in core thickness, skin thickness and construction material. Manufacturing defects, while rare, can be of several types and, most importantly, impact damage can vary greatly depending on the nature of the impacting object and its speed relative to the panel it strikes. For these reasons it is important to have a detection technique that provides a variety of standard settings but that also allows considerable variation of the detection parameters to create new detection programs.

As set out in the present paper, we now have a good understanding of the way in which a pitch-catch sensor operates to detect weaknesses and other irregularities in composite panels and in particular how such a probe can give information about the position, size and nature of impact damage. Since the measured results are highly frequency-dependent, it is generally appropriate to use a broadband technique for an initial scan and then to refine the probe pulse to give more information about the detected damage.

The CSIRO baNDIcoot sensor is mechanically robust, compact, and convenient for use in the field. Its built-in software provides a variety of standard programs that can be used by the operator and these provide informative pictorial results that allow defects to be easily identified and characterised. At a higher level, the program also allows experienced operators to vary all the excitation and analysis parameters involved and to store these to produce a new detection protocol should this become necessary because of changes in materials or conditions.

Acknowledgement

From its beginning until her sudden death in 2003, this project was under the leadership of Dr Suzanne Thwaites, and she contributed a great deal of the scientific insight essential for its success. We are also grateful to Norm Clark for his work on the early stages of the project before his retirement. These early stages, involving laser scanning, were supported financially by a contract from Boeing Commercial Airplanes, and Boeing has maintained an interest in the development of the baNDIcoot scanner and provided much useful advice. We have been grateful for the interest of the British Defence organisations DERA and DSTL and their commercial offshoot QinetiQ, and also that of the Royal Australian Air Force, over many years.

References

- [1] Cawley P, Adams R. The mechanics of the coin-tap method of non-destructive testing. *J Sound Vibr* 1988;122:299–316.
- [2] Smith RA. Advanced NDT of composites in the United Kingdom. *Mater Eval* 2007;65:697–710.
- [3] Adams RD, Cawley P. A review of defect types and nondestructive testing techniques for composites and bonded joints. *NDT Int* 1988;21(4):208–22.
- [4] Cawley P. Low frequency NDT techniques for the detection of disbonds and delaminations. *Br J NDT* 1990;32:454–61.
- [5] Lange YuV, Moskovenko IB. Low frequency acoustic nondestructive test methods. *Sov J NDT* 1979;15:788–97.
- [6] Lange YuV. *Akusticheskie nizkочастотные методы и средства контроля многослойных конструкций* (Acoustic low frequency methods and tools for testing multilayered structures). Moscow: Mashinostroyeniye; 1991.
- [7] Skudrzyk E. *Simple and complex vibratory systems*. University Park, PA: The Pennsylvania State University Press; 1968.
- [8] Soedel W. *Vibrations of shells and plates*. 2nd ed. New York: Marcel Dekker; 1993 [chapter 15].
- [9] Thwaites S, Clark NH. Non-destructive testing of honeycomb sandwich structures using elastic waves. *J Sound Vibr* 1995;187:253–69.
- [10] Clark NH, Thwaites S. Local phase velocity measurements in plates. *J Sound Vibr* 1995;187:241–52.
- [11] Fletcher NH, Thwaites S. Propagant phase in reverberant environments. *J Acoust Soc Am* 1996;99:314–23.
- [12] Nelson LJ, Dalton RP, Birt EA, Jones LD, Smith RA. A new low frequency technique for blind-side inspections. *Insight* 2006;48:149–54.
- [13] Dickinson LP, Thwaites S. Characterisation of soft impact damage in composite panels using a “pitch-catch” acoustic probe. *Acoustics Australia* 1999;27:37–40.
- [14] Dickinson LP, Thwaites S. Bandicoot—a novel approach to using a pitch-catch acoustic probe for field non-destructive testing. *Acoustics Australia* 2002;30:93–6.
- [15] Agilent Technologies. Data sheet ADNS-601X DS 27 May 2005.
- [16] Rossing TD, Fletcher NH. *Principles of vibration and sound*. 2nd ed. New York: Springer-Verlag; 2004 [chapter 3].
- [17] Morse PM. *Vibration and sound*. 2nd ed. New York: American Institute of Physics; 1976 [sect 20].